

Measuring the Hubble constant: gravitational wave observations meet galaxy clustering

Remya Nair,^{1,*} Sukanta Bose,^{2,3,†} and Tarun Deep Saini^{4,‡}

¹*Department of Physics, Kyoto University, Kyoto 606-8502, Japan*

²*Inter-University Centre for Astronomy and Astrophysics, Post Bag 4, Ganeshkhind, Pune 411 007, India*

³*Department of Physics & Astronomy, Washington State University,
1245 Webster, Pullman, WA 99164-2814, U.S.A*

⁴*Department of Physics, Indian Institute of Science, Bangalore 560012, India*

(Dated: February 7, 2022)

We show how the distances to binary black holes measured in gravitational wave observations with ground-based interferometers can be used to constrain the redshift-distance relation and, thereby, measure the Hubble constant (H_0). Gravitational wave observations of stellar-mass binary black holes are not expected to be accompanied by any electro-magnetic event that may help in accessing their redshifts. We address this deficiency by using an optical catalog to get the distribution of galaxies in redshift. Assuming that the clustering of the binaries is correlated with that of the galaxies, we propose using that correlation to measure H_0 . We show that employing this method on simulated data obtained for second-generation networks comprising at least three detectors, e.g., advanced LIGO - advanced VIRGO network, one can measure H_0 with an accuracy of $\sim 8\%$ with detection of a reference population of 25 binaries, each with black holes of mass $10M_\odot$. As expected, with third-generation detectors like the *Einstein telescope* (ET), which will measure distances much more accurately and to greater depths, one can obtain better estimates for H_0 . Specifically, we show that with 25 observations, ET can constrain H_0 to an accuracy of $\sim 7\%$. This method can also be used to estimate other cosmological parameters like the matter density Ω_m and the dark energy equation of state.

I. INTRODUCTION

We are living in an era of precision cosmology but a complete understanding of the nature of dark energy, which is responsible for the observed late-time acceleration of the Universe, still eludes us [1]. Obtaining accurate and precise distance estimates to sources at cosmological redshifts is paramount in getting an insight into this mysterious component of the Universe. It is known that the gravitational wave (GW) signal from inspiraling compact object binaries can allow for a unique way to measure their luminosity distance with reasonably good precision, when observed with a sensitive enough GW detector network [2–4]. The detection of GW170817 in both GW and electromagnetic (EM) waves was used to determine the Hubble constant $H_0 = 70^{+12}_{-8}$ km/sec/Mpc [5].

The work we present here relies on two pillars of observational astronomy: multiple cosmological observations of the clustering of galaxies and gravitational-wave measurements. We propose a method to combine them in order to measure cosmological parameters and to understand the expansion history of the Universe. We do so after accounting for a selection effect that arises due to the fact that the sensitivity of a network of GW detectors to inspiraling binaries varies with their sky-position, orbital inclination, and distance.

Type Ia supernovae (SNeIa) are termed as ‘standard candles’ in cosmology; distance estimates obtained from their observations helped to map the cosmic expansion history of the Universe. Since different models of the Universe may predict somewhat different evolution, these distance estimates can even be used to test the validity of these models. For robust tests of these models it is desirable to have a variety of observations that probe the observable Universe in different ways. This helps in identifying and mitigating systematic errors.

In the past, measurements from a number of observations have been employed, either independently or in combination, to get estimates of cosmological parameters. These observations include (but are not limited to): SNeIa, baryon acoustic oscillations (BAO), galaxy ages, cosmic microwave background (CMB), weak lensing, etc. [6, 7]. SNeIa measurements gave the first persuasive evidence for the existence of the recent accelerated phase of the expansion of the Universe [8]. Future surveys, like the Dark Energy Survey (DES), [9], the Panoramic Survey Telescope and

*Electronic address: remya@tap.scphys.kyoto-u.ac.jp

†Electronic address: sukanta@iucaa.in

‡Electronic address: tarun@physics.iisc.ernet.in

Rapid Response System (Pan-STARRS) [10], and the Large Synoptic Survey Telescope (LSST) [11] will substantially increase the number of SNeIa candidates, but the estimates on cosmological parameters obtained from these may be limited by the systematic errors.

With so many new SNeIa discoveries, it is expected that soon the systematic uncertainties will become comparable to statistical uncertainties owing to the diminishing value of the latter with every new observation [12]. Further, it is now also understood that systematic uncertainties in SNeIa observations are correlated. Potential sources of systematics include variations of SNeIa magnitudes that correlate with the properties of their host galaxies [13], and model assumptions in the light-curve fitting methods used to standardize the SNeIa candidates [14]. An additional problem is that distance estimates obtained from SNeIa observations are indirect and depend on a distance ladder, where measurements of nearby stars are used to calibrate distances to far-off objects in a series of steps (see [15] and references therein). Any uncertainties in such a calibration can add significant errors to the distance estimate of sources at large (cosmological) distances.

Another cause of concern in finding robust constraints on cosmological parameters is the inconsistency between the parameter estimates from different cosmological probes. For example the constraints on the Hubble constant from non-local experiments, like the CMB measurements of the Planck satellite [16], have been in significant tension with the results of the Hubble space telescope (HST) [17]. The latest Planck High Frequency Instrument (HFI) data [18], confirmed and further increased this tension. Its latest estimate of H_0 is 66.93 ± 0.62 km/sec/Mpc (68% confidence level) against the improved HST estimate of 73.00 ± 1.75 km/sec/Mpc (68% confidence level) [19]. Hence the inconsistency in the estimate of the Hubble constant now stands at a staggering $> 3\sigma$ confidence level (assuming standard Λ cold dark matter (LCDM) cosmology). The tension can be somewhat abated by considering an extended LCDM scenario and allowing for phantom equation of state for dark energy, but the tension resurfaces upon the addition of BAO or SNeIa data [20]. Moreover, disagreement between distance estimates from BAO and SNeIa measurements have been reported in the past [21]. In such a scenario, having a new observational window to view the Universe is very appealing.

The detection of gravitational waves by the LIGO-VIRGO detector network [22–25] have ushered in the era of GW astronomy. Analogous to standard-candle SNeIa, GW measurements of inspiraling neutron star (NS) or black hole (BH) binaries can be used as ‘standard sirens’ in cosmology [26]. GW measurements will provide independent distance estimates that will complement other probes of precision cosmology mentioned earlier. Since the underlying assumptions, the observational techniques, the biases and the systematic errors of all these probes are decidedly different, the hope is that requiring consistency among them and combining them for parameter estimation will help in identifying systematic errors and model dependencies. The idea of using GW sources as standard sirens in cosmology, was initially put forward by Schutz in 1986, where it was shown that kilometer-sized GW interferometers can be used to constrain cosmological parameters, like the Hubble constant, to an accuracy of 3% using observations of coalescing NS binaries [26]. GWs from compact binary mergers can give physically calibrated absolute distances to sources at large redshifts, i.e., unlike SNeIa measurements these do not depend on a distance ladder. The calibration here lies in the assumption that general relativity accurately describes the gravitational waveform. The measurement of the wave amplitude, the frequency, the chirp rate (rate of change of frequency) and the orbital inclination angle of the binary system, from a network of GW detectors, contain information about the luminosity and brightness of the GW source. The chirp rate is a measure of the luminosity of the compact binary system since the change in frequency is caused by the energy loss through emission of GWs, and the observed amplitude is a measure of the brightness. Therefore the luminosity distance to the faraway source can be inferred from these observations.

Although the GW signals provide a direct measurement of distance, they do not provide a redshift estimate of the source, which is essential if one wants to constrain the distance-redshift relationship in cosmology. The scale-invariance of the binary black hole (BBH) waveforms with redshifted mass implies that GW signals from a local compact binary with component masses (m_1, m_2) would be indistinguishable from the GW signal from a compact binary at a redshift z with component masses $(m_1/(1+z), m_2/(1+z))$. Hence, to use these distances in cosmology one requires an independent measure of redshift. Identifying the host galaxy is one way this information can be obtained. That would, however, require good localization of the GW source in the sky.

The projected sky localisation accuracy of a three-detector network comprising ground-based detectors of Advanced LIGO (aLIGO) and Advanced VIRGO (AdV) [27, 28], operating at their respective design sensitivities, can range from about a tenth of a sq. deg. to a few tens of sq. deg. with median value of a few sq. deg. (at 68% confidence) for a BBH with total mass of $20M_\odot$ and at a luminosity distance of 1 Gpc [2, 3, 22, 25, 29]. Thus, a few square-degrees is a reasonable estimate for localisation accuracy of a second-generation three-detector network for a range of source masses similar to those of the BBHs already observed in GWs. Since such a sky patch can contain thousands of galaxies, the chances of identifying the host galaxy of a GW event from a galaxy catalog can be dismal.

Note that the latest NS-NS discovery by the LIGO-VIRGO network was accompanied by an extensive follow-up effort by around 70 ground- and space-based observatories which observed the sky localisation patch given by the GW signal across the electromagnetic spectrum. This led to the discovery of the first EM counterpart to a GW event [30].

It is difficult to say at this time whether there would be many such NS-NS events in the future or if we just got lucky this time (given that the event was very near at ~ 41 Mpc). For the foreseeable future these kind of EM-counterpart detections will be limited to low redshifts. Nevertheless, the angular resolution is expected to get better in the future with the addition of KAGRA [31] and LIGO-India [32] in the network, but even then the probability of identifying the host galaxy for far redshift sources unambiguously, may remain small.

The main aim of this work is to show how the distances measured from GW observations of binary black holes with ground-based interferometers can be used to constrain the redshift-distance relation and hence estimate the Hubble constant. After showing how this idea can be implemented in a realistic scenario with the aLIGO-AdV three-detector network, we also demonstrate the improvement in accuracy that can be achieved with observations of the same systems in the third-generation observatory in the form of the Einstein Telescope (ET) [33]. We begin in the next section with a synopsis of a variety of approaches that have been applied in the past to determine the redshift of the GW standard candles.

II. PROPOSALS FOR OBTAINING COSMOLOGICAL PARAMETERS FROM GW SOURCES

Various methods have been proposed to constrain cosmological models using GW signals from coalescing binaries. We recapitulate the ones most relevant to our method here.

A. Electro-magnetic counterpart to the GW event

The most straightforward way to measure the redshift associated with a GW event is to identify its EM counterpart. Gamma ray bursts (GRBs) are powerful beams of radiation lasting a few seconds, and are mainly classified into two categories: long GRB that lasts for more than two seconds and short GRB that typically lasts for less than two seconds. The nature of the short GRB has been disputed for very long [34] but the observation of GRB 170817A has confirmed binary neutron star mergers as a progenitor of short GRBs [35]. The assumptions of evolutionary processes on the formation of NS-NS/NS-BH compact binaries, the metallicity models, the star formation rates, etc., all have notable effects on the estimates of the merger rates of these compact binaries. Hence the merger rates have fairly uncertain theoretical estimates and they are poorly constrained from observations. For example the detection rates for binary NS mergers were projected to range from 0.4 to 400 events per year with advanced LIGO (aLIGO) design sensitivity in Ref. [36], but might reduce following the observation of GW170817. For BBH sources the detection rates in the same reference were projected to be in the range from 0.4 to 1000 events per year, but have been revised to be in the (narrower) range from 2 to 600 $\text{Gpc}^3\text{yr}^{-1}$ [37]. Although EM counterparts are not expected from BBH binary mergers, NASA's Fermi telescope detected a GRB 0.4 seconds after GW150914. The GRB lasted for 1 second [38] and is possibly not connected with the GW source [39, 40].

The EM follow up of GW inspiral events is a challenging task [41]. What adds to the demanding exercise of detecting a possibly highly beamed and short-lived signal, is the contrast between the sky localization accuracy of current GW networks and the fields of view of optical telescopes. The localisation provided for the GW events observed so far is poor, *viz.* ~ 100 s of sq. deg. (the sky localisation for the first GW detection had an area of 600 sq. deg.). Comparing this with the fields of view of optical telescopes like the Zwicky Transient Facility (47 sq. deg.), the Dark Energy Camera (3 sq. deg.) and the LSST (9.6 sq. deg.) gives an idea about the formidable challenge faced by astronomers in following up these events. Since the EM signals could be short lived and may peak within hours (or faster), successful EM follow up would require accurate sky localizations within a time scale of minutes to hours. To this end, many algorithms have been developed or are in development to account for telescope pointing limitations, finite observation time, the rising or setting of the target at the observatory location, etc. [41]. As mentioned in the introduction, the LIGO-VIRGO network has already detected an event, GW170817, with confirmed EM counterparts [5, 30]. Moreover, future GW networks will have narrower sky localization regions, as mentioned above. However, it is still premature to say at this time whether there would be many such NS-NS events in the future. Nevertheless multiple studies have been performed assuming simultaneous observations of the GWs and EM signatures to constrain cosmological parameters like the Hubble constant [42].

B. Neutron star mass distribution

The knowledge about the intrinsic mass distribution of the NS population can also be used to estimate source redshifts [43]. The GW signals give an estimate of the redshifted mass of the binary $m_z = m(1+z)$ and if the distribution of NS masses is known, one can obtain a distribution of the source redshift. The number of detected

pulsar binaries have steadily increased in recent years and current observations estimate that the mass distribution of NS in binary NS systems could be multi-modal where the two modes in the distribution are expected to be associated with different NS formation channels. The idea has been explored in multiple publications [44] but depends on the knowledge of NS mass distribution and may be prone to systematics from selection biases. To complicate things further, the mass distribution in double NS systems may be different from that in other systems with a single neutron star [45].

C. Tidal deformation of the neutron star

The correction to the GW waveform due to the finite size of the compact object in a binary system depends on the equation of state as well as the rest masses. If these corrections can be measured from GW signal they will provide information not just about the redshifted mass but also the rest mass of the system, hence providing an estimate of the redshift. The idea has been explored in the literature and it was shown that as small as 10% error on redshift estimate can be expected [46]. Here too the analysis depends on the knowledge of equation of state of the NS, which is highly model dependent and hence prone to systematic errors.

D. Statistical techniques with galaxy catalogs

The technique that is closest to our approach in this work is the use of existing galaxy catalogs. Schutz [26] proposed the use of sky position-luminosity distance confidence regions informed from GW measurements and statistically ruling out galaxies that did not host the event. The method has been modified and developed further in a number approaches, e.g., a Bayesian framework that incorporates assumptions and prior information about a GW source within a single data analysis framework [47], using clustering of galaxies to statistically extract the redshift information from a GW sample without identification of host galaxies for individual events [48], and using sources with known redshifts to iteratively solve for the redshift of unresolved sources [49]. The method we present here can be considered as a natural extension of [47, 48]

III. METHODOLOGY

Stellar-mass BBHs are expected to reside in galaxies or their neighborhood. Therefore, we assume that their spatial distribution follows that of galaxies. If the galaxies were uniformly randomly distributed in volume, then these sources of GWs¹ would also have been distributed in the same manner. In that case, due to the absence of spatial features in the distribution of GW sources and galaxies, the two point-sets would be uncorrelated. In reality, due to gravitational instability, galaxies show strong clustering on length-scales below about 100 Mpc. The spatial clustering of galaxies in the (z, θ, ϕ) space would then correspond to a distribution of GW sources in the (D_L, θ, ϕ) space. Therefore, while matching the patterns in the two distributions — assuming they are coincident, since BBH sources are located in and around galaxies — a method to associate z with D_L can be obtained. This would lead to the distance-redshift relation for such objects. However, it is clear that if the angular location of BBHs as GW sources is not narrow enough, then one is compelled to sample the angle-averaged galaxy clustering. Owing to the angle averaging the distribution now depends only on the redshift of the galaxies (or equivalently on D_L for GW sources). This blunts the impact of the galaxy clustering owing to the overlapping in the redshift space of clustering in different directions. The important thing to note is that the near-future GW experiments have an angular resolution, which although not enough to single-out an individual galaxy as the source of a GW event, is nonetheless sharp enough to probe the clustering length of about 100 Mpc in the nearby universe [50].

To explore the efficacy of this idea, we need to simulate GW sources taking into account their spatial clustering. Since we are assuming that the sources reside in and around galaxies, this can be done most effectively by using galaxy redshift catalogs. For our purpose we make use of the existing galaxy catalog: the Sloan Digital Sky Survey (SDSS) [51]. In Fig. 1 we show the redshift distribution of three random SDSS patches of 3, 10 and 30 sq. deg.. We chose these regions randomly from the sky area covered by SDSS and we have not employed any mass (luminosity)

¹ In this work, by GW sources we always mean BBH, and by BBH we always imply a binary of stellar-mass black holes that is a source of GWs for ground-based detectors. For obtaining the results we set the mass of each black hole in every binary to $10 M_\odot$. We leave it for future work to study how different black hole mass distributions affect these results.

cuts on the galaxies in this work. The galaxy distribution will change if the patches are narrowed to a tenth of a square degrees or broadened to a few hundreds of square degrees. Very narrow and very broad patches will reduce the power of the method described here since both types will limit the optimal use of galaxy clustering information (more about this below). We expect our qualitative results to hold as long as the sky patches are no larger than 30 sq. deg.. We further emphasize that these numbers do not represent the ‘optimal’ sky patch area. A much detailed analysis can be carried out to study the effect of patch size on the estimates. We leave this exercise for future. Although the SDSS is not a complete all-sky catalog, it is wide enough to sample several sky patches of the size that typical angular resolution for a GW source necessitates. We are also constrained by the sensitivity of the near-future GW experiments, and the limiting redshift probed by the SDSS falls neatly in that range. The formalism described here would require a more complete all-sky galaxy redshift catalog for use in the near-future experiments than what exists today.

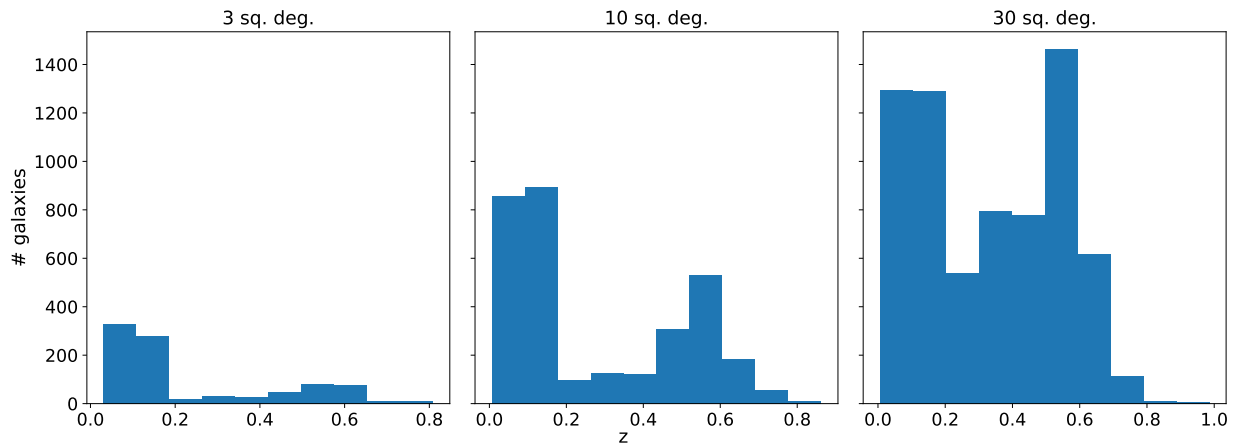


FIG. 1: The redshift distribution of galaxies in three random sky patches from the SDSS catalog.

A. Bayesian formulation

The goal of this section is to formulate a method for extracting cosmological information from GW sources when their redshifts are not known. We do this by first constructing the Probability Distribution Function (PDF) for cosmological parameters in the most general case. We subsequently use reasonable simplifications to produce an approximate PDF that is used to test the efficacy of our method.

The spatial location of a GW source, given by its angular position and luminosity distance, can be determined only up to a limited precision that depends on its redshift, GW luminosity, orientation, sky position, and the detector network [2]. The measured angular position of the source and its luminosity distance would in general be given by a likelihood function that is obtained from an analysis of GW data by marginalizing all parameters other than those that determine the location of the source in three-dimensional space. Broadly speaking, for loud enough BBH events as GW sources this distribution can be expected to peak in a certain direction $\Omega_0 \equiv (\theta_0, \phi_0)$ and at a certain luminosity distance $D_L = D_0$, and then fall-off away from the peak roughly at a rate that depends on the sensitivity of the detector configuration and the nature of the source and its physical parameters.

To infer cosmological parameters from GW observations one needs to relate them to such a likelihood function. Given the choice of cosmology, the source redshift z_s , and source angular coordinates Ω_s , the likelihood function can be expressed as

$$P(\mathcal{S} | z_s, \Omega_s, \xi) = \mathcal{L}(\Omega_s, D_L(z_s, \xi)) , \quad (1)$$

where ξ represents the parameters of the cosmological model, and \mathcal{S} , as a shorthand for (standard) siren, represents the GW data.

If the location of the source (z_s, Ω_s) is known, the likelihood function is sufficient to constrain the cosmology, although we would need a large number of GW sources to better constrain cosmological parameters ξ . Assuming that the GW signal is not accompanied by an electromagnetic counterpart, this information (z_s) would in general not be available to us. However, if we assume that the GW source originates inside a galaxy (hitherto unknown to us), then

the least we know is that the source position would coincide with the location of that galaxy. In fact, without any more information at hand, we know *only* that the source resides in *one* of the galaxies in the universe.

We proceed by assuming that all the galaxies in the universe are equally likely to host the source of our GW signal. If we know the redshift and angular position of *all* the galaxies in the sky, the Bayesian prior PDF for the source parameters (z_s, Ω_s) can be written as

$$P_s(z_s, \Omega_s) \propto \sum_i \delta(z_s - z_i) \delta^2(\Omega_s - \Omega_i), \quad (2)$$

where the sum is over *all* the galaxies in the universe, and the omitted normalization constant is $1/N_g$, where N_g is the total number of galaxies in the Universe. Note that although this is formally correct, in practice we need only those galaxies that are roughly in the direction of the source, as we argue in a following section (§ III B). The two-dimensional delta function can be written explicitly as

$$\delta^2(\Omega_s - \Omega_i) = \frac{\delta(\theta_s - \theta_i) \delta(\phi_s - \phi_i)}{\sin(\theta_s)}, \quad (3)$$

where θ and ϕ are the usual spherical polar coordinates to locate galaxies on the celestial sphere. The denominator in this expression comes about since this is probability density per unit solid angle. If the galaxy redshifts are not known precisely but contain Gaussian noise, and the angular positions of galaxies are known precisely, then we can write P_s as

$$P_s(z_s, \Omega_s) \propto \sum_i \exp \left[-\frac{(z_s - z_i)^2}{2\sigma_i^2} \right] \delta^2(\Omega_s - \Omega_i), \quad (4)$$

where σ_i is the error in the redshift of the i^{th} galaxy. Even when this error is small, it is useful to choose the Gaussian spread to be somewhat large since it helps to make the discrete galaxy distribution into a more continuous one and, thereby, help in a more meaningful correlation with a GW source distribution. We discuss this point more in § IV. We have omitted the normalization constant above, and shall continue to do so below.

Without any other available information we can assign this as the prior PDF for (z_s, Ω_s) . However, not all galaxies are equally likely to host GW events; in fact, we expect the probability that a certain galaxy is the source of our GW signal to be at least proportional to its mass, or its type (spiral or elliptical). Also, if the detector configuration is insensitive to GW sources beyond a certain distance, we can use this information to further reduce the number of galaxies required for the construction of our prior PDF $P_s(z_s, \Omega_s)$. Therefore, in general, we modulate the prior distribution P_s with a weight function W_i affixed to the i th galaxy inside the summation sign to take into account additional astrophysical/detector information. This weight function determines the likelihood of the i^{th} galaxy to be the host of the GW source. We show this explicitly in the next section.

If the prior PDF for the cosmological parameters is $P_c(\xi)$, then the complete prior joint PDF is given by

$$P(z_s, \Omega_s, \xi) = P_s(z_s, \Omega_s) P_c(\xi). \quad (5)$$

Using the Bayes theorem we can now write the posterior PDF for (z_s, Ω_s, ξ) in terms of the likelihood function and the prior PDF as

$$P(z_s, \Omega_s, \xi | \mathcal{S}) \propto P(\mathcal{S} | z_s, \Omega_s, \xi) P(z_s, \Omega_s, \xi). \quad (6)$$

After marginalizing this over the source parameters (z_s, Ω_s) we obtain

$$P(\xi | \mathcal{S}) \propto \int dz_s d\Omega_s P(\mathcal{S} | z_s, \Omega_s, \xi) P(z_s, \Omega_s, \xi). \quad (7)$$

For the prior source distribution given by Eq. (2), the integrals can be done analytically to give

$$P(\xi | \mathcal{S}) \propto \sum_i \mathcal{L}(\Omega_i, D_L(z_i, \xi)) P_c(\xi), \quad (8)$$

and if the prior source distribution is given by Eq. (4) then we obtain

$$P(\xi | \mathcal{S}) \propto \int dz_s \sum_i \left(\exp \left[-\frac{(z_s - z_i)^2}{2\sigma_i^2} \right] \mathcal{L}(\Omega_i, D_L(z_s, \xi)) P_c(\xi) \right),$$

where the integral over redshift can be converted to an integral over distance. Henceforth, we work with this posterior.

Till now in our formulation we have considered only a single GW source. Noting that the posterior PDF in the last equation $P(\xi|\mathcal{S})$ can be used as a prior PDF for another source, we can easily combine data from different GW events. Formally, if $\{\mathcal{S}_{\text{new}}\} = \{\mathcal{S}, \mathcal{S}_{\text{old}}\}$ then

$$P(\xi|\mathcal{S}_{\text{new}}) \propto \int dz_s \sum_i \left(\exp \left[-\frac{(z_s - z_i)^2}{2\sigma_i^2} \right] \mathcal{L}(\Omega_i, D_L(z_s, \xi)) P(\xi|\mathcal{S}_{\text{old}}) \right).$$

Note that \mathcal{S}_{old} contains all the GW sources analyzed till the point the new source \mathcal{S} is added to create the updated data set \mathcal{S}_{new} . This recursion can be easily used to obtain a single expression for the combined data, but is notationally somewhat cumbersome. To investigate the efficacy of this method using simulated data, however, we make simplifications by approximating the likelihood function as an error-box in the following section.

B. Approximate likelihood function

Note that although in our formulation, thus far, the sum is over *all* the galaxies in the sky, in practice the dominant contribution comes only from the galaxies that are in directions where the likelihood function is significant. Moreover, if prior information is also assumed for the cosmological parameters, a rough measure of the redshift of the source is then known, and only galaxies with redshift close to that value would contribute to this sum. To see this more clearly, let us assume that our likelihood function is approximately given by

$$\begin{aligned} \mathcal{L}(\Omega, D_L) &\propto \exp \left[-\frac{(D_L - D_0)^2}{2\sigma_D^2} \right], \text{ for } \Omega \in \Delta\Omega, \\ &= 0, \text{ for } \Omega \notin \Delta\Omega. \end{aligned} \quad (9)$$

Here we have assumed that the measured luminosity distance $D_L = D_0$ with standard deviation σ_D , and the angular location of the source is somewhere inside the solid angle $\Delta\Omega$, with all directions inside this solid angle being equally likely. Since the angular position Ω is not explicitly present in the likelihood function, the posterior distribution for ξ takes the form

$$P(\xi|\mathcal{S}) \propto \int dz_s \left(\exp \left[-\frac{(D_L(z_s, \xi) - D_0)^2}{2\sigma_D^2} \right] \times n_s(z_s) P_c(\xi) \right)$$

with

$$n_s(z_s) \propto \sum_{\Omega_i \in \Delta\Omega} W_i \exp \left[-\frac{(z_s - z_i)^2}{2\sigma_i^2} \right], \quad (10)$$

where W_i is a weight function that may be chosen to be the likelihood of the i^{th} galaxy to be the host of the GW source. For example, this may depend on galaxy type, galaxy mass or other astrophysical parameters that determine the rate of GW events in these galaxies. One also needs to account for detector characteristics: some events will be easier to observe than others because, e.g., they are located at a nearby redshift, have an optimal sky position, or have their orbital plane favorably oriented. On the other hand, this function, or even the full prior, may be chosen to be uninformative. For the illustration of our method below, we opt to use an informed prior.

1. On the completeness of galaxy catalogs

It is worth mentioning that although till this point our formulation seemingly requires a complete catalog of galaxies in the universe, it is in fact not necessary. This can be argued in general, but it is easier to argue from the point of view of this approximate formulation as follows. The redshift information required to determine cosmology from luminosity distance is encoded in the source function $n_s(z_s)$. If this function is featureless, then essentially we gain no useful knowledge about the redshift of the source by knowing this function. However, since galaxies are strongly clustered on various length-scales, the distribution of galaxy in space is full of features, such as peaks and troughs in redshift arising due to clusters and voids. If the sample of galaxies is not complete, i.e., it does not contain *all* the existing galaxies in a given direction, but still captures the dense regions in sufficient detail, then the informative content of galaxy clustering in $n_s(z_s)$ can suffice to constrain cosmology, and in fact can be looked at as pattern matching between galaxy clusters and GW source clusters. However, for the truest match one should use the most complete galaxy catalog available.

IV. NUMERICAL SIMULATIONS

To test the efficacy of this method we simulate GW data by using the projected GW source configurations for near-future experiments using the distribution of galaxy redshifts from SDSS. For simplicity, we use the approximate formalism of § III B. Since the redshift depth of the current experiments is likely to remain shallow, at the most such observations will be able to constrain the Hubble constant. The luminosity distance for a flat LCDM model is given by

$$D_L(z) = \frac{c(1+z)}{H_0} \int_0^z \frac{dz'}{\sqrt{\Omega_m(1+z')^3 + (1-\Omega_m)}}, \quad (11)$$

where Ω_m is the matter density, c is the speed of light, and H_0 is the Hubble constant. For our analysis we fix the matter density to the input value $\Omega_m = 0.3$ and do parameter estimation only for H_0 .

The analysis in the previous section was carried out in the redshift space. We find it convenient to do our calculations in the distance space. For this purpose, note that in Eq. (10), the combination $n_s(z_s)dz_s = dN$ is proportional to the number of galaxies in the redshift interval dz_s , which is a pure number. This combination can be expressed in the distance space through $n_s(z_s)dz_s = n_s(z_s(D))dD$, where $D = D_L(z_s, \xi)$. Therefore, for a given cosmology, we translate the galaxy redshifts to luminosity distance using Eq. (11) and construct the number density function in the distance space. Therefore, Eq. (10) is modified to

$$P(H_0 | \mathcal{S}) \propto \int dD \quad \left(\exp \left[-\frac{(D - D_0)^2}{2\sigma_D^2} \right] \times n_s(D)P_c(H_0) \right),$$

where

$$n_s(D, H_0) \propto \frac{1}{\sum_i W_i} \times \sum_{i, \Omega_i \in \Delta\Omega} \frac{W_i}{\sigma_{D_i}} \exp \left[-\frac{(D - D_L(z_i, H_0))^2}{2\sigma_{D_i}^2} \right]. \quad (12)$$

Above, $\Delta\Omega$ represents a patch in the sky that can vary in location and area for different GW sources [52], and $W_i \equiv W(D_i)$ is the aforementioned weight function that determines the likelihood of the i^{th} galaxy to be the host.

In the present work, we do not exhaust accounting for the various potential astrophysical effects on W_i . For example, we assume that all galaxies, regardless of their size, luminosity and type, are equally likely hosts of BBHs. Although this is not a realistic assumption, it provides a simple framework to describe our method. We, however, account for the detector characteristics of the aLIGO-AdV three-detector network and calculate the fraction of GW sources ($10 M_\odot + 10 M_\odot$ BBH mergers) that will be detected in different sky patches and at varying depths. We average over the BBH orbital orientations in space in order to obtain this detection fraction. The resulting $W(D_i)$ is plotted as a function of distance for one of the sky patches in Fig. 2.

Selection effects will indeed affect the above posterior by influencing the integrand through the density of detected BBHs at varying depths. The way we simulate this is detailed below. Its imprint on the posterior appears through the normalization, as was shown in a general setting studied in Ref. [53].

The spectroscopic redshifts of galaxies are obtained with high precision. Consequently, the derived luminosity distance errors from galaxy catalog are much smaller compared to the distance errors expected from GW measurements. In the limiting case where the error-bars are very small, it is clear that using the actual error-bars on the distance would result in a very fluctuating distribution. The two point-set distributions, obtained from the galaxies and the GW sources, are best compared in a coarse-grained manner. Therefore, instead of using the inferred distance error for galaxies, we use a $\sigma_{D_i}/D_L(z_i, H_0) = 10\%$ for all galaxies, consistent with what we stated earlier. However, the distance error for GW sources in our simulations, σ_D/D_0 is taken to be their respective measurement error, as explained below.

For our calculations, $P_c(H_0)$, the prior probability for the Hubble parameter, is assumed to be uniform between 40-100 km/sec/Mpc. The sources are combined as before using the recursion for $\{\mathcal{S}_{\text{new}}\} = \{\mathcal{S}, \mathcal{S}_{\text{old}}\}$ using

$$P(H_0 | \mathcal{S}_{\text{new}}) \propto \int dD \quad \left(\exp \left[-\frac{(D - D_0)^2}{2\sigma_D^2} \right] \times n_s(D)P(H_0 | \mathcal{S}_{\text{old}}) \right).$$

The upper limit on the integral is informed from the mock GW sample generated. For most patches D_{max} is chosen to be ~ 3500 Mpc for the aLIGO-AdV network and ~ 4500 Mpc for ET network. Note that $n_s(D)$ comprises different sets of galaxies for different GW sources since these sources will, in general, be in different directions. To summarize our method we list below the steps one can follow to obtain the posterior distribution for H_0 :

1. Obtain the probability distribution over D from GW measurements. Note that, as mentioned earlier, in the realistic case one would obtain a distribution over both Ω and D , but for simplicity we use the distribution as given in Eq. (9).
2. For each GW observation, obtain the galaxy distribution $n_s(D)$ from a sky-patch taken from the SDSS catalog that has support in the BBH distribution obtained in step 1 (e.g., a sky patch in the direction of the BBH source with area similar to $\Delta\Omega$).

In our simulations, the sky localization error has the spread mentioned in §. I ($\Delta\Omega \in [3, 30]$ sq. deg.). However, whenever this error is less than 3 sq. deg., one can reset $\Delta\Omega$ to be equal to 3 sq. deg. and retain those BBHs for further analysis. BBHs with errors greater than 30 sq. deg. can be dropped. Note that as stated earlier, we cite these number because we have confirmed the robustness of our method for these localisation areas. They are not claimed here to be ‘optimal’ values of the sky patch area.

3. Assume a prior for H_0 . This could be either a uniform prior over some allowed range of admissible H_0 values or can be an informed prior coming from some other cosmological observations (e.g. Planck or HST measurements).
4. The weighting function $W(D_i)$ used in this work is purely dependent on GW detection efficiency, and does not depend on the galaxy distribution in any way. For every sky-patch of interest, we populate it uniformly on that section of the sphere with 10-10 M_\odot BBHs, such that there are 1600 sources in every distance bin. This number does not correspond to any realistic distribution of BBHs but is chosen merely to ensure that the error in detection probability estimated at each distance bin is less than 3% (absolute). Additionally, we allow the cosine of the inclination angle to vary over 100 uniformly spaced values for every source. The SNR of each source is computed at each detector and only when it is above 8 in at least two of them and the network SNR is 10 or higher do we classify it as detected. This is how we compute the detection probability in distance bins of 10 Mpc, in the range $D \in [50, 4500]$ Mpc. Note that it varies from one sky patch to another because the antenna-patterns of the detectors (and even the network antenna pattern [54]) vary across the sky. A geometric explanation for this weighting function is given in Ref. [55]. (Additionally, we compute the network SNR of each source, and the average network SNR in each distance bin, which is used in the distance error estimation described below.)
5. Plug these three distributions and the weighting function in Eq. (12) to obtain the posterior over H_0 .
6. Combine the posterior distribution obtained from all the GW measurements to obtain the final $P(H_0|S)$.

Note that in general one can obtain the posterior over any number of cosmological parameters. In this work we have assumed a simple flat Λ CDM model with two free parameters: H_0 and Ω_m , and we fix $\Omega_m = 0.3$. In a future work we will also consider Ω_m and possibly the dark energy equation of state. Since we do not have enough GW observations to test our method, we work with a simulated GW catalog as also mentioned earlier. In the next subsection we discuss how we simulate this GW catalog and also outline the key steps to obtain $P(H_0|S)$ in this case.

A. GW catalog: Second generation detectors

We now describe the method adopted for producing realistic catalogs of GW sources for near-future detector configurations. As mentioned earlier, we assume that the BBH sources are associated with galaxies. To get the galaxy samples we chose different sky patches from the SDSS database. Our sky patches were obtained from a conical search (limited in redshift and solid-angle), in the SDSS catalog. In principle one can choose from a variety of shapes for the sky patch, but in this first study we chose this simple shape to focus more on the main idea behind the method.

The first step to construct the GW catalog is to obtain the weight function $W(D)$. This was outlined in the previous section. The detector characteristics (e.g. the noise sensitivity), the distance to the source and its sky position, and the orientation of the plane of the binary with respect to the detector, all play an important role in determining whether the event will be detected by the GW detectors and hence in determining $W(D)$ (see, e.g., Refs. [54, 56] and the references therein). Note that in this work we have studied a particular population of BBH sources, but the analysis can be extended to other kinds of binary sources, such as NS-BH or NS-NS systems; moreover, BBH with somewhat higher masses will provide smaller error at any given redshift and more redshift depth.

To obtain the weight function $W(D)$ mentioned above, we evaluate what fraction of our BBH population (which is randomly oriented in space to create a realistic population) will have SNRs above a threshold value in our detector-network of interest. We set this threshold such that the SNR is at least 8 in two of the three detectors and the network SNR is at least 10. This criterion is used to estimate what fraction of BBH sources at some distance will be detectable in GWs. We take the distance error to be 30% for a BBH at a network SNR of 20 [2–4]. For a BBH signal

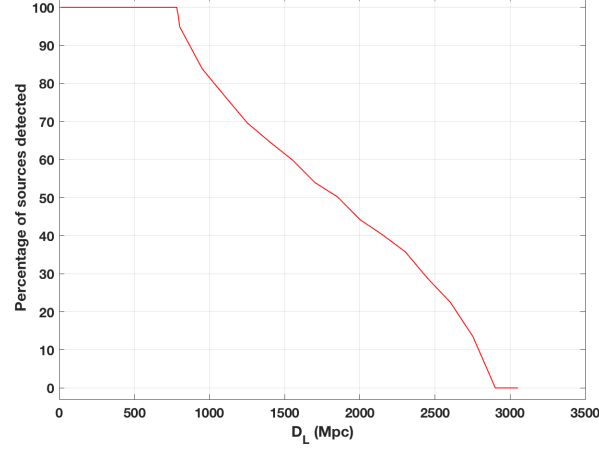


FIG. 2: The weights $W(D_i)$ assigned to the galaxies in a single sky patch is plotted as a function of distance for one of the sky patches for the aLIGO-AdV network.

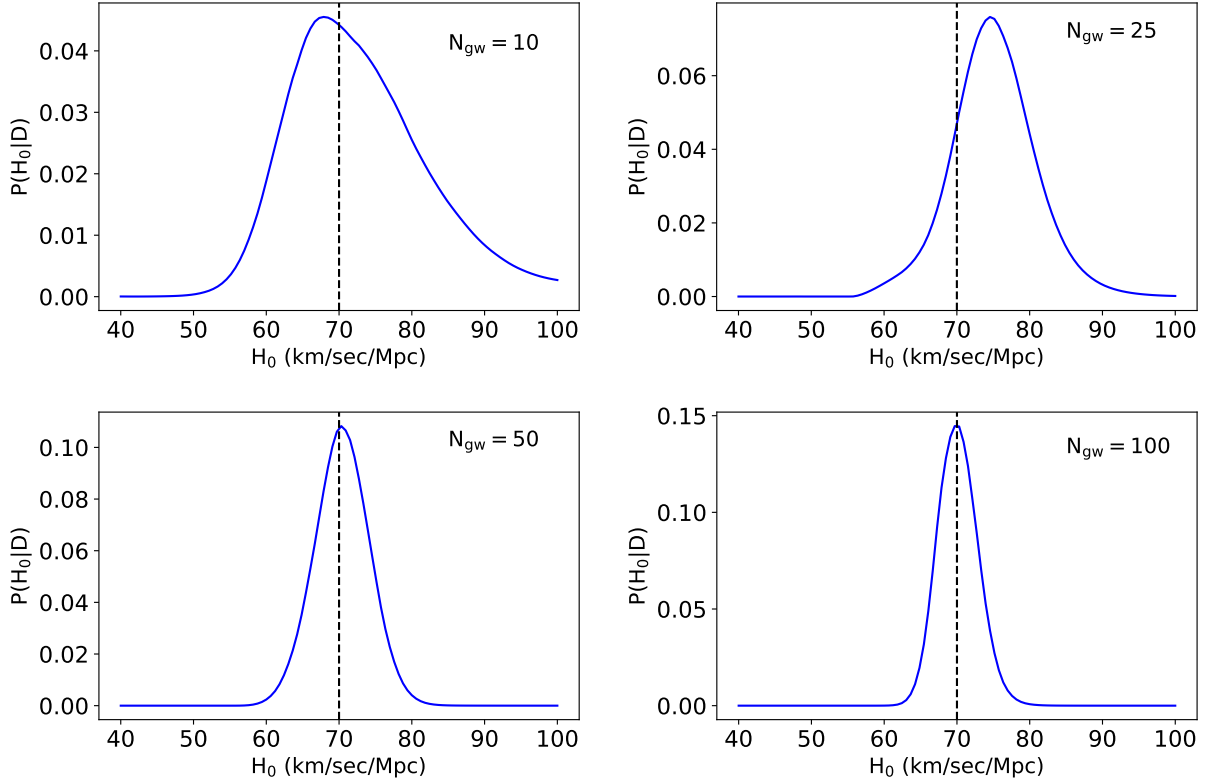


FIG. 3: The plots show the projected normalized posterior probability distribution for H_0 obtained from the aLIGO-AdV network. Dashed line at 70 km/sec/Mpc, represents the value of H_0 used for simulation (fiducial input). The number of GW sources used, is mentioned in each panel. The value of H_0 at the peak of the posterior distribution is (clockwise from upper-left panel) 67.8 km/sec/Mpc, 74.6 km/sec/Mpc, 70.3 km/sec/Mpc and 70.0 km/sec/Mpc respectively. For all plots the sky patches have localisation error $\Delta\Omega \in [3, 30]$ sq. deg..

with network $\text{SNR} = \rho$, its percentage distance error scales roughly as $30\% \times (20/\rho)$. For ET, the fraction of BBHs detected, remains 100% to a greater distance than that corresponding to the second generation aLIGO-AdV network. Moreover, the SNR of the same BBH is about 10 times higher, and distance error about 10 times lower, in ET than in aLIGO-AdV. Once we have the fraction of BBH sources that are detectable by the GW network as a function of

N_{GW}	H_0 (aLIGO-AdV)	H_0 (ET)
10	$67.8^{+12.0}_{-6.1}$	$69.1^{+8.2}_{-9.9}$
25	$74.6^{+5.7}_{-5.4}$	$75.3^{+4.9}_{-5.1}$
50	$70.3^{+4.1}_{-3.6}$	$68.2^{+3.1}_{-2.9}$
100	$70.0^{+2.7}_{-2.8}$	$70.1^{+2.6}_{-2.3}$

TABLE I: The table shows the estimated values of the Hubble constant in units of km/sec/Mpc, from the aLIGO-AdV network (second column), and the ET network (third column) along with error-bars obtained by considering the threshold value for $P(H_0 | \mathcal{S})$ that encloses 68% probability region around the peak of the distribution. Different rows show different number of GW sources. The binaries are simulated to have random orientations, and the distance errors are determined by averaging over the orientations.

distance, we use it to obtain $P(H_0 | \mathcal{S})$ as outlined below:

1. In the sky patch of interest, say we have N galaxies distributed over some redshifts.
2. Map all the redshifts to distances using Eq. (11) where H_0 is now a free parameter ($\Omega_m = 0.3$). We assign each galaxy a weight based on what fraction of BBH sources to its distance would be detectable by the GW detector network (see Fig. 2). Next we construct the distance distribution for the galaxies as in Eq. (12).
3. Assume a prior distribution over H_0 . Here we use a uniform prior over 40-100 km/sec/Mpc.
4. Now, we go back to the galaxy redshift catalog and select a galaxy randomly, so any of the N galaxies is equally likely to be picked.
5. Say, the chosen galaxy falls in the j^{th} bin. We put a BBH source in this galaxy with a probability f_j , where f_j is the fraction of detectable sources at that distance (this is done by throwing a uniform random number q between $[0, 1]$ and putting a source in the galaxy if $f_j > q$).
6. Once we have the BBH source, we first map its redshift to a ‘true’ distance D_m (evaluated from Eq. (11)) by assuming $\Omega_m = 0.3$ and $H_0 = 70$ km/sec/Mpc. We also know what is the expected SNR of this BBH merger and we translate that to an error (σ_D) on the distance as discussed earlier in this subsection.
7. We randomly sample from a Gaussian distribution, centered at D_m and with standard deviation equal to the distance error, both obtained in the previous step.
8. Once we have the ‘observed’ D_0 and the corresponding error we construct the probability distribution for this ‘measurement’ (Eq. (9)).
9. Now that we have all the required probability distributions we plug them in Eq. (12) to obtain the posterior over H_0 .

Note that, as mentioned earlier, the weights assigned to galaxies depend on the direction of the sky patch (as GW detectors do not have isotropic efficiency). The weights given to the galaxies, for the three-detector aLIGO-AdV network, as a function of redshift for one of the sky patches is shown in Fig. 2. In the figure one can see that the weight drops substantially beyond a distance of ~ 2000 Mpc. This drop occurs because of the SNR threshold we set on the GW events [55].

B. GW catalog: Third generation detector

We next apply the same method to a third generation detector like the Einstein Telescope (ET) [33] to see how these estimates will change if the same BBH sources are obtained with much higher SNRs. We assume a triangular configuration for ET as discussed in [57] with three interferometers located at the same sites as LIGO-Hanford, LIGO-Livingston and Virgo, respectively.. The way the catalog is generated is the same as in the previous section but instead of aLIGO-AdV the Einstein Telescope is used as a GW detector-network. Unlike the second generation

detectors, ET will observe the same BBH sources with much smaller distance errors. It will also detect sources to larger redshifts (in a future work, we plan to study ET BBH sources to analyze how well ET may be able to constrain the dark energy equation of state [42]). A plot similar to Fig. 2 would show 100% sources recovered to distances of ~ 5000 Mpc.

V. RESULTS

Once we know how to populate the GW catalog using the SDSS galaxies as hosts we generate multiple such catalogs with varying number of GW sources. These sources are then assigned distances and distance errors, and the galaxies are also weighted to account for the detection efficiency of the GW detectors, using the method outlined in the sections § III and § IV. Once we have these distributions we estimate the posterior distribution of the cosmological parameters given the (mock-)GW data (Eq. (12)).

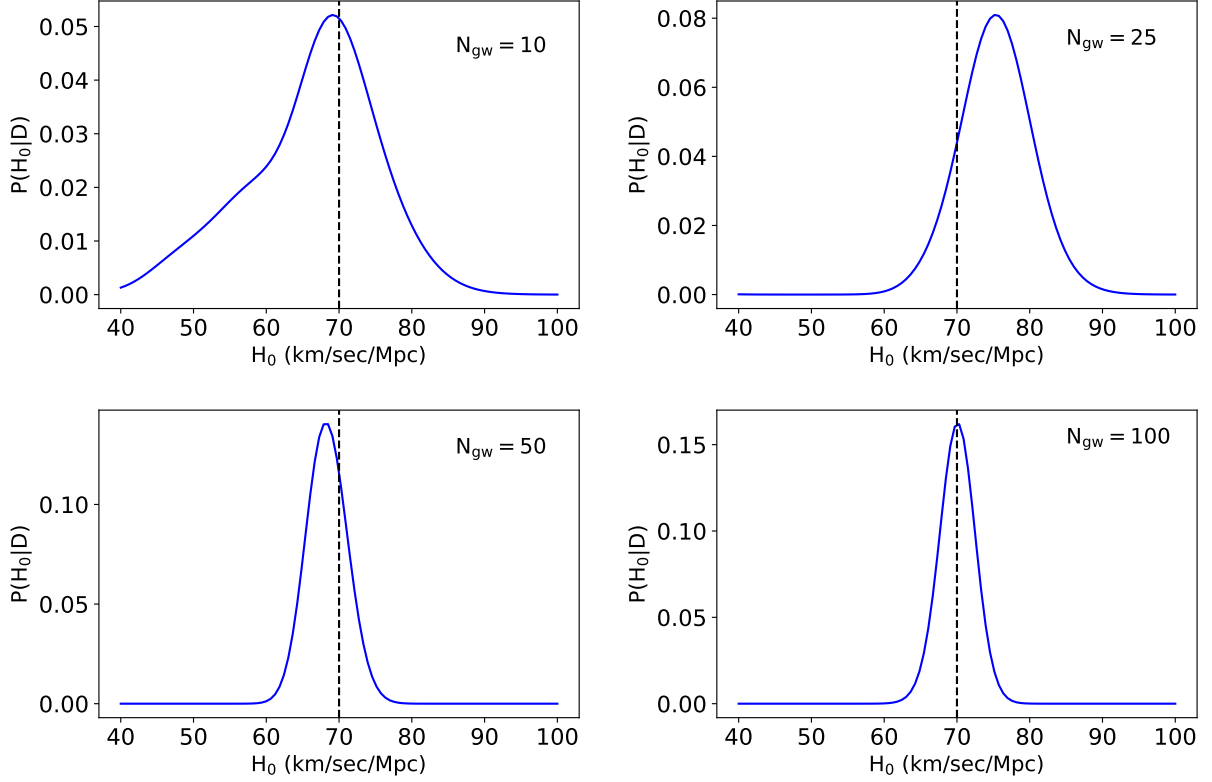


FIG. 4: The plots show the normalized posterior probability distribution for H_0 obtained from the third generation detector ET. Dashed line at 70 km/sec/Mpc, represents the value of H_0 used for simulation (fiducial input). The number of GW sources used, is mentioned in each panel. The value of H_0 at the peak of the posterior distribution is (clockwise from upper-left panel) 69.1 km/sec/Mpc, 75.3 km/sec/Mpc, 68.2 km/sec/Mpc and 70.1 km/sec/Mpc respectively. For all plots the sky patches have localisation error $\Delta\Omega \in [3, 30]$ sq. deg..

We perform the analysis for aLIGO-AdV network as well as for a third generation ET network. Note that the estimates and plots shown are from a particular set of sky patches and a specific realization of the GW catalog. The estimate and the posterior distribution of H_0 will be different for a different setting. The results will converge for large number of GW sources.

Results obtained for the second generation detector network are shown in Table I and Fig. 3. We estimate the posterior distribution for H_0 using varying number of GW sources and we report the H_0 value that corresponds to the peak of the posterior distribution. We also quote error-bars obtained by considering the threshold value for $P(H_0|\mathcal{S})$ that encloses 68% probability region around the peak of the distribution. With the aLIGO-AdV network we find that one can constrain H_0 with an accuracy of $\sim 8\%$ with as few as 25 GW sources. The integral in Eq. (12) would peak for the value of H_0 for which the GW probability distribution in D (Eq. (9)) has maximum overlap with the probability distribution in D obtained from galaxies (Eq. (12)). Note that when there are multiple regions of

comparable clustering in the galaxy distribution, the posterior in H_0 can be multi-modal. But this problem can be addressed by combining multiple GW measurements. Combining measurements is similar to stacking histograms and we expect that eventually, a peak emerges around the correct value of H_0 .

Results obtained by repeating the analysis for a third generation detector (ET) network are also shown in Table I and in Fig. 4. In this case we find that H_0 is constrained to an accuracy of about 7% with 25 GW sources. Note that in this case since we can go much deeper in redshift, we can also get estimates of parameters like Ω_m (which we have fixed to 0.3 here), or the equation of state for dark energy (in the case of non- Λ CDM models). But at higher redshifts, the incompleteness of the galaxy catalog may potentially be a problem and one would have to address this in the formulation more carefully. We leave this exercise for future work.

VI. DISCUSSION

GW signals from coalescing binaries will provide distance measurements that are complementary to the electromagnetic standard candle measurements used to constrain cosmological parameters. Additionally these measurements do not suffer from the calibration error that is one of the major systematic uncertainties that plagues the supernovae measurements. (Note that GW detectors are affected by intrinsic calibration uncertainties that are at present no more than 10% in strain amplitude and 10° in phase [23]. Efforts are on, however, to reduce these errors [24].) But doing cosmology with inspiraling binaries requires the use of data obtained from EM surveys since GW measurements from these binaries alone can not provide redshift information of the source, which is imperative to constrain the distance-redshift relation. Some of these GW sources (like NS-NS mergers) are expected to have EM counterparts, and a coordinated EM observation of the source can obtain redshifts for these events, as was done for the NS-NS event observed by the LIGO-VIRGO network. But this method will not work for mergers that are not accompanied by an electromagnetic event, for electromagnetic events that are too short-lived, or for very far off sources. Many methods have been suggested in the past to address this problem, as discussed in the introduction.

In this work we proposed to use the spatial clustering of galaxies, as seen through many large-scale surveys, to infer the spatial clustering of GW sources. We have introduced a general Bayesian formulation for extracting cosmological information using GW observation and galaxy clustering data. The general formulation takes into account the possibility of complex constraints on spatial location of GW sources, which includes angular location as well as distance information. The formulation was then simplified to ascertain the efficacy of this technique by generating simulated GW data. This mock GW catalog was generated using the galaxies from the SDSS survey as ‘host’ galaxies. For this work we considered only $10 M_\odot + 10 M_\odot$ BH-BH binaries. The GW sources were then analyzed with the SDSS galaxies as the hosts of GW events.

We estimated the posterior distribution of the Hubble parameter H_0 by analyzing the expected GW measurements from second generation detector network aLIGO-AdV, where we included the information about the orientation of the binary, sky position, detector characteristics, etc., and we found that one can constrain H_0 with an accuracy of $\sim 8\%$ with just 25 sources (Fig. 3). Third generation detectors like the Einstein Telescope will see the same sources with much higher SNR and, therefore, smaller distance errors. It will also detect sources to larger redshifts. Here, however, we restricted ET observations to BBH sources up to a similar depth, specifically, with $z \leq 0.6$ and we showed that measurements from the third generation detector will be able to constrain H_0 to an accuracy of $\sim 7\%$ with 25 detections (Fig. 4).

Hence we have shown that it should be possible to obtain excellent constraints on the Hubble parameter with the near-future GW detector configurations. However, the same technique could be used for future experiments to extract the matter density parameter (Ω_m) or properties of dark energy, like the equation of state etc. This would be possible when the data acquires more precision and sufficient redshift depth.

While working on this paper we came across Ref. [58], which is somewhat similar in spirit to this work in that the author sets constraints on cosmological parameters by using the cross-correlation between observations from ET and the Euclid survey. We would like to note that in addition to giving constraints for the current second generation ground-based detectors, our treatment is more realistic since we also take into account the detector characteristics in detail.

Note that we have made many simplifying assumptions in this work. We have assumed that the spatial distribution of our GW sources (BBH) is identical to that of galaxies. In reality, the merger rates of coalescing binaries may depend in some hitherto unknown manner on the source galaxies. For example, the number of GW sources in a galaxy should scale with the number of stars in a galaxy, so our assumption that each galaxy contributes equally to the galaxy distribution function may not translate to it contributing equally to the GW source function. This can be taken into account if we utilize information about the luminosity of a galaxy, which we can use while assigning how much it contributes to the galaxy source function. However, it is likely that the GW rates could also depend on the galaxy type, i.e., on whether the galaxy is spiral or elliptical. Since spiral and elliptical galaxies cluster differently,

this would have an impact on parameter estimation. Considering that any sufficiently prominent peak of galaxy cluster would roughly contain an equal mixture of different types of galaxies, and the fact that our method extracts maximum information from the dominant peaks in the galaxy distribution, to zeroth order our method should work fine. However, to obtain more detailed information (such as parameters of dark energy) from this method would require addressing these issues in some detail. This is beyond the scope of this investigation and will be followed up in a future work.

Furthermore an addition that may become important in the future for an analysis like this is the information from population synthesis models. These models predict the source mass distribution for NS-NS, NS-BH or BBH binaries. They also predict merger rates for these binaries. But since most of these models are degenerate and a large number of GW detections are required to narrow in on some preferred model, we have not included them in the current analysis. A further important improvement may come from all-sky galaxy catalogs. Since GW detectors are not directional, a coalescing binary can be observed in most parts of the sky. This is more true for GW detector networks. Even so, it may happen that some sources fall in sky areas that are not covered by galaxy surveys yet. In such a case we will not be able to use such GW signals in our analysis. These and other issues will be addressed in a future work.

Acknowledgments

We thank the anonymous referee for suggesting useful changes to the manuscript which have improved our analysis significantly. We would also like to thank Varun Sahni, Sheelu Abraham, Timothee Delubac, Takahiro Tanaka and John Veitch for discussions at various stages of this project. We thank Will Farr and Archisman Ghosh for carefully reading the manuscript and making several useful suggestions. RN acknowledges the support of the Japan Society for the Promotion of Science (JSPS) fellowship, Grant No. 16F16025. RN also thanks the Inter University Centre for Astronomy and Astrophysics (Pune) for hospitality, where part of this work was done. This work is supported in part by NSF grants PHY-1206108 and PHY-1506497, and the Navajbai Ratan Tata Trust. We made use of the publicly available data from SDSS. Funding for the SDSS and SDSS-II has been provided by the Alfred P. Sloan Foundation, the Participating Institutions, the National Science Foundation, the U.S. Department of Energy, the National Aeronautics and Space Administration, the Japanese Monbukagakusho, the Max Planck Society, and the Higher Education Funding Council for England. The SDSS Web Site is <http://www.sdss.org/>. The SDSS is managed by the Astrophysical Research Consortium (ARC) for the Participating Institutions. The Participating Institutions are The University of Chicago, Fermilab, the Institute for Advanced Study, the Japan Participation Group, The Johns Hopkins University, Los Alamos National Laboratory, the Max-Planck-Institute for Astronomy (MPIA), the Max-Planck-Institute for Astrophysics (MPA), New Mexico State University, University of Pittsburgh, Princeton University, the United States Naval Observatory, and the University of Washington.

-
- [1] B. Ratra & P. J. E. Peebles, *Phys. Rev. D* **37**, 3406 (1988); C. Wetterich, *Nucl. Phys. B* **302**, 668 (1988); J. Ellis, S. Kalara, K.A. Olive & C. Wetterich, *Phys. Lett. B* **228**, 264 (1989); R. R. Caldwell, R. Dave & P. J. Steinhardt, *Phys. Rev. Lett.* **80**, 1582 (1998); V. Sahni & A. Starobinsky, *Int. J. Mod. Phys. D* **15**, 2105 (2006); E. J. Copeland, M. Sami & S. Tsujikawa, *Int. J. Mod. Phys. D* **15**, 1753 (2006); J. Frieman M. Turner & D. Huterer *Ann. Rev. Astron. Astrophys.* **46**, 385 (2008); R. R. Caldwell & M. Kamionkowski, *Ann. Rev. Nucl. Part. Sci.* **59**, 397 (2009); T. Clifton, P. G. Ferreira, A. Padilla & C. Skordis *Phys. Rep.* **513**, 1 (2012).
 - [2] P. Ajith & Sukanta Bose, *Phys. Rev. D* **79**, 084032 (2009).
 - [3] A. Ghosh, P. Ajith & W. del Pozzo *Phys. Rev. D* **94**, 104070 (2016).
 - [4] S. Nissanke, D. E. Holz, S. A. Hughes, N. Dalal, & J. L. Sievers *Astrophys. J.* **725**, 496 (2010).
 - [5] B. P. Abbott et al., *Nature* **551** 85 (2017).
 - [6] D. H. Weinberg, M. J. Mortonson, D. J. Eisenstein, C. Hirata, A. G. Riess, & E. Rozo, *Phys. Rep.* **530** (2), 87 (2013).
 - [7] R. Amanullah et al., *Astrophys. J.* **716**, 712 (2010); A. Lewis & S. Bridle, *Phys. Rev. D* **66**, 103511 (2002); M. J. Mortonson, D. Huterer & W. Hu, *Phys. Rev. D* **82** 063004 (2010); C. Blake et al., *Mon. Not. Roy. Astr. Soc.* **418**, 1707 (2011); L. Anderson et al., *Mon. Not. Roy. Astr. Soc.* **427**, 3435 (2012); U. Seljak, A. Makarov, R. Mandelbaum, C. M. Hirata, N. Padmanabhan, P. McDonald, M. R. Blanton, M. Tegmark, N. A. Bahcall, J. Brinkmann, *Phys. Rev. D* **71**, 043511 (2005).
 - [8] Supernova Search Team collaboration: A. G. Riess et al., *Astronom. J.* **116**, 1009 (1998); Supernova Cosmology Project collaboration: S. Perlmutter et al., *Astrophys. J.* **517**, 565 (1999).
 - [9] www.darkenergysurvey.org
 - [10] www.pan-starrs.ifa.hawaii.edu
 - [11] www.lsst.org
 - [12] A. Conley et al., *Astrophys. J. Suppl.* **192**, 1 (2011); D. Scolnic et al., *Astrophys. J.* **795**, 45 (2014); J. Newling, B. Bassett, R. Hlozek, M. Kunz, M. Smith & M. Varughese, *Mon. Not. Roy. Astr. Soc.* **421** (2), 913 (2012).

- [13] P. L. Kelly, M. Hicken, D. L. Burke, K. S. Mandel, R. B. Kirshner, *Astrophys. J.* **715**, no. 2 743 (2010).
- [14] R. J. Foley et al., *Astronom. J.* **143**, no. 5 113 (2012).
- [15] W. L. Freedman et al., *Astrophys. J.* **553**, no. 1 47 (2001).
- [16] P. A. R. Ade et al. (Planck collaboration), *Astron. Astrophys.* **571** A1 (2014).
- [17] A. G. Riess, L. Macri, S. Casertano, H. Lampeitl, H. C. Ferguson, A. V. Filippenko, S. W. Jha, W. Li, R. Chornock, *Astrophys. J.* **730**, 119 (2011) Erratum: *Astrophys. J.* **732**, 129 (2011).
- [18] Planck Collaboration: N. Aghanim et al., *Astron. Astrophys.* **596**, A107 (2016).
- [19] A. G. Riess et al., *Astrophys. J.* **826** 56 (2016).
- [20] E. D. Valentino, A. Melchiorri & J. Silk, *Phys. Lett. B* **761**, 242 (2016).
- [21] W. J. Percival, S. Cole, D. J. Eisenstein, R. C. Nichol, J. A. Peacock, A. C. Pope & A. S. Szalay, *Mon. Not. Roy. Astr. Soc.* **381**, 1053 (2007); R. Lazkoz, S. Nesseris & L. Perivolaropoulos, *JCAP* **07** 012 (2008).
- [22] B. P. Abbott et al., *Phys. Rev. Lett.* **116**, 061102 (2016);
- [23] B. P. Abbott et al., *Phys. Rev. Lett.* **116**, 241102 (2016);
- [24] B. P. Abbott et al., *Phys. Rev. D* **95**, 062003 (2017);
- [25] LIGO Scientific Collaboration and Virgo Collaboration: B. P. Abbott et al., *Phys. Rev. Lett.* **116**, 241103 (2016); B. P. Abbott et al., *Phys. Rev. Lett.* **118**, 221101 (2017); B. P. Abbott et al., *Phys. Rev. Lett.* **119**, 141101 (2017); B. P. Abbott et al., *Phys. Rev. Lett.* **119**, 161101 (2017); B. P. Abbott et al., *Astrophys. J. Lett.* **851** L35 (2017).
- [26] B. F. Schutz, *Nature* **323**, 310 (1986).
- [27] <http://ligo.org>
- [28] <http://www.virgo-gw.eu>
- [29] LIGO Scientific Collaboration and Virgo Collaboration: B. P. Abbott et al., *Astrophys. J.* **826**, no.1, L13 (2016).
- [30] LIGO Scientific Collaboration and Virgo Collaboration: B. P. Abbott et al., *Astrophys. J. Lett.* **848** 2 (2017).
- [31] KAGRA Collaboration: Yoichi Aso et al., *Phys. Rev. D* **88**, 043007 (2013).
- [32] C. S. Unnikrishnan, *Int. J. Mod. Phys. D* **22**, 1341010 (2013).
- [33] <http://www.et-gw.eu>
- [34] N. Tanvir, A. J. Levan, A. S. Fruchter, J. Hjorth, R. A. Hounsell, K. Wiersema & R. L. Tunnicliffe, *Nature* **500**, 547 (2013); E. Berger, W. Fong & R. Chornock, *Astrophys. J. Lett.* **774** L23 (2013).
- [35] LIGO Scientific Collaboration, Virgo Collaboration, Fermi Gamma-Ray Burst Monitor, INTEGRAL, *Astrophys. J. Lett.* **848** L13 2017
- [36] J. Abadie et al., *Class. Quant. Grav.* **27**, 173001 (2010).
- [37] B. P. Abbott *et al.* [LIGO Scientific and Virgo Collaborations], *Astrophys. J.* **833**, no. 1, L1 (2016) doi:10.3847/2041-8205/833/1/L1 [arXiv:1602.03842 [astro-ph.HE]].
- [38] V. Connaughton et al., *Astrophys. J. Lett.* **826** L6 (2016).
- [39] A. Loeb, *Astrophys. J. Lett.* 819 L21 (2016).
- [40] V. Savchenko et al., *Astrophys. J. Lett.* **820**, L36 (2016)
- [41] L. P. Singer et al., *Astrophys. J. Lett.*, **829** L15 (2016); B. P. Abbott et al., *Astrophys. J. Lett.* **833** L1 (2016); M. Coughlin, & C. Stubbs, *Experimental Astronomy* **42** 165 (2016); J. Rana, A. Singhal, B. Gadre, V. Bhalerao, & S. Bose, *Astrophys. J.* **838** 108 (2017); V. Srivastava, V. Bhalerao, A. P. Ravi, A. Ghosh & S. Bose, *Astrophys. J.* **838** 46 (2017); M. L. Chan, Y. M. Hu, C. Messenger, M. Hendry, & I. S. Heng, *Astrophys. J.* **834** 84 (2017).
- [42] D. E. Holz & S. A. Hughes, *Astrophys. J.* **629**, 15 (2005); N. Dalal, D. E. Holz, S. A. Hughes, & B. Jain, *Phys. Rev. D* **74**, 063006 (2006); K. G. Arun, B. R. Iyer, B. S. Sathyaprakash, S. Sinha & C. Van Den Broeck, *Phys. Rev. D* **76**, 104016 (2007); C. Cutler & D. E. Holz, *Phys. Rev. D* **80**, 104009 (2009); B. S. Sathyaprakash, B. F. Schutz & C. Van Den Broeck, *Class. Quant. Grav.* **27** 215006 (2010); C. Van Den Broeck, M. Trias, B. S. Sathyaprakash, & A. M. Sintes, *Phys. Rev. D* **81**, 124031 (2010); S. Nissanke, D. E. Holz, S. A. Hughes, N. Dalal, & J. L. Sievers, *Astrophys. J.* **725**, 496 (2010); S. Nissanke, D. E. Holz, N. Dalal, S. A. Hughes, J. L. Sievers & Christopher M. Hirata, *arXiv:1307.2638*.
- [43] D. Markovic, *Phys. Rev. D* **48**, 4738 (1993).
- [44] D. F. Chernoff & L. S. Finn, *Astrophys. J. Lett.* **411**, L5 (1993); L. S. Finn, *Phys. Rev. D* **53**, 2878 (1996); S. R. Taylor, J. R. Gair & I. Mandel, *Phys. Rev. D* **85**, 023535 (2012).
- [45] B. Kiziltan, A. Kottas, M. De Yoreo, & S. E. Thorsett, *Astrophys. J.* **778**, 66 (2013); F. Ozel, D. Psaltis, R. Narayan & A. S. Villarreal, *Astrophys. J.* **757**, 55 (2012).
- [46] C. Messenger & J. Read, *Phys. Rev. Lett.* **108**, 091101 (2012).
- [47] W. Del Pozzo, *Phys. Rev. D* **86**, 043011 (2012).
- [48] C. L. MacLeod & C. J. Hogan *Phys. Rev. D* **77**, 043512 (2008).
- [49] T. D. Saini, S. K. Sethi & V. Sahni, *Phys. Rev. D* **81**, 103009 (2010).
- [50] H. Y. Chen and D. E. Holz, *arXiv:1712.06531 [astro-ph.CO]*.
- [51] S. Alam et al., *Astrophys. J. Suppl.* **219**, 12 (2015).
- [52] H. Y. Chen, D. E. Holz, J. Miller, M. Evans, S. Vitale and J. Creighton, *arXiv:1709.08079 [astro-ph.CO]*.
- [53] I. Mandel, W. Farr & J. Gair, LIGO Document P1600187, <https://dcc.ligo.org/LIGO-P1600187/public>.
- [54] A. Pai, S. Dhurandhar and S. Bose, *Phys. Rev. D* **64**, 042004 (2001).
- [55] S. Ghosh and S. Bose, *arXiv:1308.6081 [astro-ph.HE]*.
- [56] S. Bose, T. Dayanga, S. Ghosh & D. Talukder, *Class. Quant. Grav.* **28** 134009 (2011).
- [57] W. Zhao, C. Van Den Broeck, D. Baskaran, & T. G. F. Li *Phys. Rev. D* **83**, 023005 (2011).
- [58] M. Oguri, *Phys. Rev. D* **93**, 083511 (2016).